Desalination and Water Treatment
www.deswater.com
doi: 10.1080/19443994.2016.1159988

57 (2016) 26136–26152
November

Taylor & Francis
Taylor & Francis Group

Simultaneous removal of phenol and cyanide from aqueous solution by co-culture of strain immobilized onto coconut shell activated carbon

Neetu Singh*, Chandrajit Balomajumder

Department of Chemical Engineering, Indian Institute of Technology, Roorkee, India, emails: neeturbs@gmail.com (N. Singh), chandfch@iitr.ernet.in (C. Balomajumder)

Received 20 August 2015; Accepted 22 February 2016

ABSTRACT

In this study, the simultaneous biosorption and bioaccumulation of phenol and cyanide by co-culture/mixed culture of *Pseudomonas putida* (MTCC 1144) and *Serratia odorifera* (MTCC 5700) strains immobilized onto coconut shell activated carbon (CSAC) were investigated. The batch experiments were performed for the elimination of phenol and cyanide from mono and binary aqueous solution using initial concentrations of phenol (100–1,000 mg/L) and cyanide (10–100 mg/L). Under optimum conditions, the CSAC was demonstrated a biosorption capacity 500.55 mg/g of phenol and 2.41 mg/g of cyanide at pH 8, biomass dose 30 g/L and temperature 30˚C. In a binary component system among six multicomponent isotherms, extended Freundlich model indicates a better fit for both phenol and cyanide. Moreover, the kinetic experimental results show that both phenol and cyanide were defined by the pseudo-first-order kinetic model. Thermodynamic study was established that the simultaneous biosorption and bioaccumulation of phenol indicates the exothermic nature of the process and cyanide indicates the endothermic nature of the process.

Keywords: Co-culture; Cyanide; Phenol; Multicomponent isotherm; Kinetics; Thermodynamics

1. Introduction

It is well predictable that the occurrence of phenol and cyanide compounds in the atmosphere can be unfavorable to a diversity of living species, as well as to man. Phenol, cyanide, and their compounds are generally present in the effluent generated from a variety of industries including metal processing, metal electroplating, pharmaceuticals, iron-steel, coke, mining, petroleum refining, pesticide, electroplating, pharmaceuticals, wood conserving chemicals, plastics, and explosives manufacturing industries [1–7]. Presence of phenol and cyanide in effluent is extremely dangerous, and in the simultaneous occurrence, the influences are increased. Long-term contact of phenol and cyanide can cause nerve damage, thyroid effects, weight loss, eyes and skin injuries, gastrointestinal disorders, liver, lung, kidney and heart damage, even death, and other severe mental disturbances [8,9]. The minimal national standard (MINAS) of the Central Pollution Control Board (CPCB) and United States of Environmental Protection Agencies (USEPA), regulations for industrial wastewater set the maximum contamination limit (MCL) of phenol and cyanide at 0.5 and 0.2 mg/L, respectively [2,4].

*Corresponding author.

The foremost methods, which have been employed to reduce the phenol and cyanide from wastewater, comprise chemical oxidation, precipitation/coagulation, biosorption, biodegradation, ion exchange, electrolytic methods, and membrane processing etc. These techniques have been established to be insufficient, because they involve high operational and capital costs and may also be related to the production of secondary pollutants. Among them, biosorption method is effective in usage comprised the use of biosorbents. Biosorption has emerged as a favorable method, having advantages as low cost, high removal efficiency, easy operation, no additional nutrient requirements, and no harmful effects on the environment. A wide range of bacteria, fungi, byproducts, and agricultural waste has been discovered for the elimination of pollutants [2,4,10]. The use of micro-organisms immobilized onto biosorbent surface for the removal of organic species provides a possible alternative to accessible treatment technique for detoxification of toxic components from industrial effluents. Bioaccumulation process has different advantages such as: no chemical sludge formation, extra efficiency, ease of operation, and cost-effectiveness. Enhancement of the biosorption capacity of carbon in the biological method has been known to bioregeneration, that is, the improvement of biosorption capacity of biosorbent by the bioaccumulation process. Removal of pollutants by biological method on the biosorbent surface can reopen biosorption sites [11]. It has been commonly established that bioregeneration process involves desorption of adsorbed pollutants from biosorbent to bulk solution, followed through bioaccumulation. The use of simultaneous biosorption and bioaccumulation processes is to be very effective in the elimination of toxic compounds from different types of wastewater [12,13]. Many researches on bioregeneration techniques have focused on a monocomponent only. On the other hand, wastewater generally contains more than one component that might affect treatment methods.

The present study is based on the simultaneous removal of phenol and cyanide by co-culture of micro-organisms immobilized onto surface of coconut shell activated carbon (CSAC). However, the foremost aim of this current study is (i) to define the optimum value of process parameters viz., biosorbent dose, pH, contact time, temperature, initial concentration of phenol and cyanide for simultaneous elimination of phenol and cyanide by the use of co-culture of *Pseudomonas putida* (MTCC 1144) and *Serratia odorifera* (MTCC 5700) immobilized onto the surface of CSAC (ii) to define the parameters of monocomponent and multicomponent adsorption isotherms models, (iii) to study the thermodynamics of the process, and (iv) to evaluate the kinetics of simultaneous biosorption and bioaccumulation of phenol and cyanide and find out the best fit kinetic models.

2. Materials and methods

2.1. Preparation of biosorbent

Coconut shell obtained was thoroughly washed with distilled water to remove dirt residue on the surface, and then carbonization of coconut shell was carried out at 600˚C in a muffle furnace for 2 h [14,15]. After pretreatment, dried CSAC was then transformed into particle size < 2 mm by crushing in a grinder and sieving. CSAC was soaked with 2 N H_2SO_4 solution in 2:1 liquid–solid ratio and stirred at 60˚C until complete removal of water obtained. The treated CSAC was washed with distilled water to eliminate excess acid and dried in an oven at 80˚C for overnight. This CSAC was kept in a sealed storage bag and used as a carrier for micro-organism. Co-cultures of *P. putida* (MTCC 1194) and *S. odorifera* (MTCC 5700) were used in this experimental study of simultaneous biosorption and bioaccumulation.

2.2. Preparation of biosorbate solutions and chemicals

For the current study, phenol and cyanide were obtained from Himedia Laboratories Pvt. Ltd. Mumbai, India. All reagents used were of the analytical grade. Stock solutions of phenol and cyanide were obtained by dissolving the appropriate quantities of phenol and sodium cyanide in 1 L of double-distilled water, respectively. Stock solution of both components was prepared daily as per necessity. The solution was kept in a brown bottle of glass, and entirely enclosed with aluminum foil to avoid photo-oxidation. The pH of the solutions was regulated using dilute HCl and NaOH. Surface morphology and characterization of biosorbent were determined using Field Emission Scanning Electron Microscopy (Fe-SEM), Energy-Dispersive X-ray (EDX), and Fourier Transform Infrared Spectroscopy (FTIR). Fourier Transform Infrared Spectroscopy (FTIR, Nicolet 6700, USA) was employed to determine the functional groups existing on biosorbent's surface. Field Emission Scanning Electron Microscope (FE-SEM Quanta 200 FEG, FEI Netherlands) was employed to determine the surface morphology and chemical composition of the element present on the surface of CSAC. The samples of immobilized co-culture were subjected to vacuum condition monitored by the application of 15 kV. The SEM, EDX, and FTIR study was performed at three stages, namely before simultaneous biosorption, after

immobilization of co-culture, and after the phenol and cyanide biosorption. The surface area (BET) of the biosorbent was calculated by physisorption surface analysis on surface area analyzer (ASAP 2010 Micrometrics, USA).

2.3. Acclimatization of micro-organism and inoculum development

Co-culture was familiarized to phenol up to 1,000 mg/L and cyanide up to 100 mg/L. The micro-organism *P. putida* (MTCC 1194) was obtained from the Microbial Type Culture Collection and Gene Bank, Institute of Microbiology (IMTECH), Chandigarh, India, and bacterium *S. odorifera* (MTCC 5700) was isolated in a laboratory from coke wastewater [16]. These micro-organisms were revived in the same liquid medium and stored on the agar Petri dish. To escape precipitation of salts, the growth medium for micro-organism was sterilized in two portions.

Part 1: K_2HPO_4, $FeSO_4{\cdot}7H_2O$, KH_2PO_4,
Part 2: $(NH_4)_2SO_4$, $MnCl_2{\cdot}4H_2O$, $MgCl_2{\cdot}6H_2O$, $Na_2MoO_4{\cdot}2H_2O$ $CaCl_2{\cdot}2H_2O$ [17].

The pH and temperature of the growth medium therefore obtained were 8.1 ± 0.1 and 30°C. The revived co-cultures were grown in medium with glucose as a single source of carbon. The co-culture was then familiarized to phenol and cyanide environment by revealing the co-culture in a sequence of flasks (250 mL), in which the amount of glucose was continuously reduced and phenol and cyanide amount increased. For inoculum, an additional subculturing was completed, and all inoculum transfers were completed in exponential stage. The growth medium for micro-organism contained phenol/cyanide as the sole source of carbon and nitrogen [18]. All inoculations were achieved under aseptic environment in laminar air flow unit (Rescholar Equipment M. no. RH-57-02, Ambala, India). The growth curve of co-culture was achieved by centrifuging the cultivated cells of co-culture at 8,000 r.p.m for 15 min. Then, the pellet was formed at the bottom of the centrifuge tube. The pellet was washed with distilled water and its optical density (OD) was detected at 600 nm at time interval of 2 h in UV Spectrophotometer (Lambada 35; PerkinElmer, MA 02451, USA). For the growth curve, the phenol and cyanide concentrations to be used were 500 and 50 mg/L, respectively.

When micro-organisms are developed using two compatible substrates, e.g. two carbon sources, they have a tendency to exhaust specially the one that tolerates a maximum growth rate which is reliable with this study where micro-organism first utilizes glucose and then phenol and cyanide [19]. In addition, glucose was completely utilized by micro-organism within 25 h, as a carbon source after that micro-organism started to utilize the phenol and cyanide. This phenomenon was known as diauxic behavior as shown in Fig. 1.

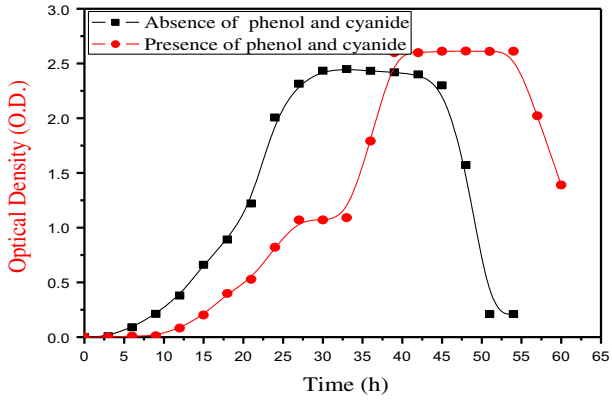

Fig. 1. Growth curve of co-culture in the absence and presence of phenol and cyanide.

2.4. Batch experimental studies

Batch experiments for simultaneous biosorption and bioaccumulation was carried out in 250-mL flat bottom flask containing 100 mL of liquid nutrient medium. All the flasks containing nutrient medium were steam sterilized in an autoclave at 121°C and 15 psi. Therefore, one loop full of micro-organism from agar plate was relocated to the autoclaved nutrient medium at room temperature in the laminar flow chamber and then retained in an incubator shaker (Metrex, MO-250, India) for 30 h at 30°C and 120 rpm for attaining maximum growth of micro-organism. After obtaining maximum growth of micro-organism, a measured quantity of CSAC was added to develop a biofilm onto biosorbent surface by keeping the nutrient solution in an incubator shaker for additional 24 h. The equilibrium study of biosorption was determined at 30°C by observing the concentration of both compounds in solution with varying initial concentration of 100–1,000 mg/L for phenol and 10–100 mg/L for cyanide until equilibrium was achieved with a fixed dose of biosorbent 30 g/L. After centrifuging, the concentration of phenol and cyanide was determined by UV Spectrophotometer with a wavelength of 510 nm for phenol and 520 nm for cyanide. For an optimization study of biosorbent dose, a fixed amount of biosorbent dose (5–60 g/L) was added to each flask. To obtain the effect of temperature and the effect of

pH, the temperature range of 20–40°C and the pH range of 4–12 were selected, respectively. Initial concentrations of phenol and cyanide were kept at 500 and 50 mg/L, respectively, excluded in those where the initial cyanide and phenol concentration effects are to be studied. All the experiments were conducted in triplicate and average results were used for the current study.

The biosorption capacity and percentage removal of phenol and cyanide were calculated by the equation given below:

$$q_t = (C_i - C_t)V/M \quad (1)$$

$$q_{eq} = (C_i - C_{eq})V/M \quad (2)$$

$$\text{Percentage removal} = ((C_i - C_f)/C_i) \times 100 \quad (3)$$

where q_{eq} is the amounts of phenol and cyanide adsorbed onto the per unit mass of biosorbent at equilibrium (mg/g), q_t is the uptake of phenol and cyanide at time t (mg/g), C_f is the final concentration of phenol and cyanide (mg/L), C_t is the liquid phase concentration of phenol and cyanide at time t (h), C_i is the initial pollutant concentration (mg/L) C_{eq} is the concentration of adsorbate at equilibrium (mg/L), V is the volume of the solution (L), M is the weight of the biosorbent (g).

3. Results and discussion

3.1. Characterization of biosorbent

Total pore volume and surface area (BET) of CSAC biosorbent was calculated by a surface area analyzer ASAP 2010 Micrometrics, USA. Before immobilization, CSAC has a high surface area (81.82 m^2/g), which confirms that it is a suitable biosorbent for the simultaneous elimination of phenol and cyanide. Figs. 2(a) and 3(a) indicate the SEM image of CSAC and co-culture/CSAC, respectively. The porous structure and smooth morphology of CSAC (Fig. 2(a)) makes it a suitable biosorbent as it improves the adsorption capacity. The occurrence of pores on the surface indicated the probability of micro-organism accumulation [20]. EDX investigation of phenol and cyanide revealed the weight percentage of chemical compositions existing on the surface of CSAC as follows: 77.93% of C, 11.63% of O, and 10.44% of S as shown in Fig. 2(b). In case of micro-organism immobilized onto the surface of CSAC as shown in Fig. 3(a), it was detected that there is a reduction in surface porosity and unevenness. The weight percentage of chemical compositions presented on the surface after immobilization was as follows: 65.1% of C, 25.81% of O, 8.04% of S, and 1.05% of Fe and EDX analysis revealed in Fig. 3(b). Fig. 4(a) characterizes the SEM image of CSAC after simultaneous biosorption and bioaccumulation. The chemical composition of the element was as follows: 47.16% of C, 35.04% of O, 10.45% of S, 3.89% of Na, and 3.46% of Fe.

FTIR of CSAC was accompanied in the range of 400–4,000 cm^{-1} for three types, namely (a) before simultaneous biosorption and bioaccumulation of phenol and cyanide, (b) after immobilization of co-culture, and (c) after simultaneous biosorption and bioaccumulation (Fig. 5). Functional groups like methyl, amide, hydroxyl, and carboxyl vibrations were existing on biosorbent and bacterial surfaces. Vibration peaks around 3,500–3,000 cm^{-1} were established as the vibra-

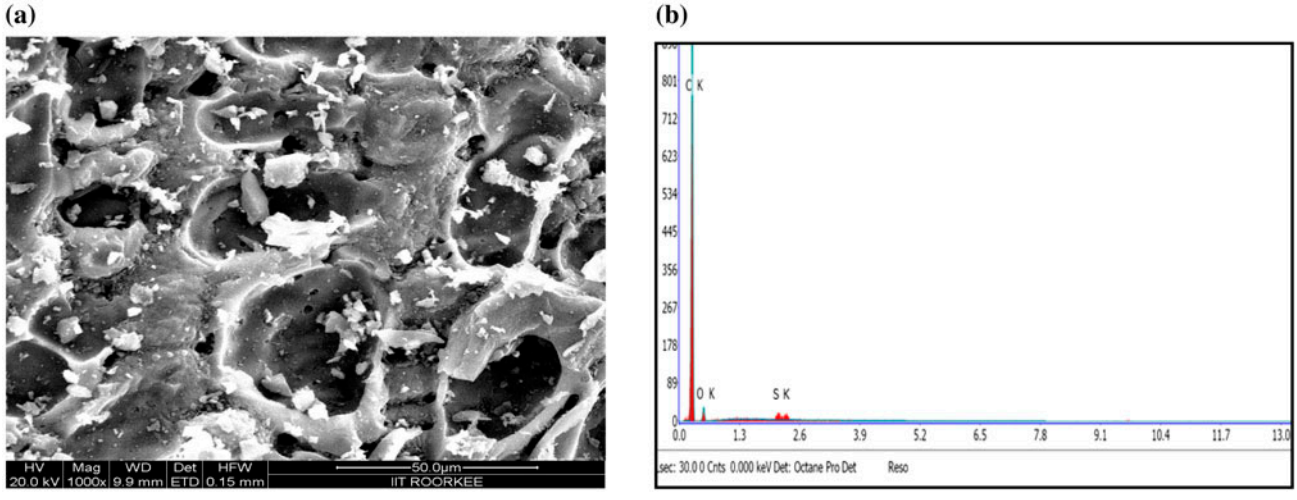

Fig. 2. (a) SEM image of CSAC before biosorption and (b) EDX analysis of CSAC before biosorption.

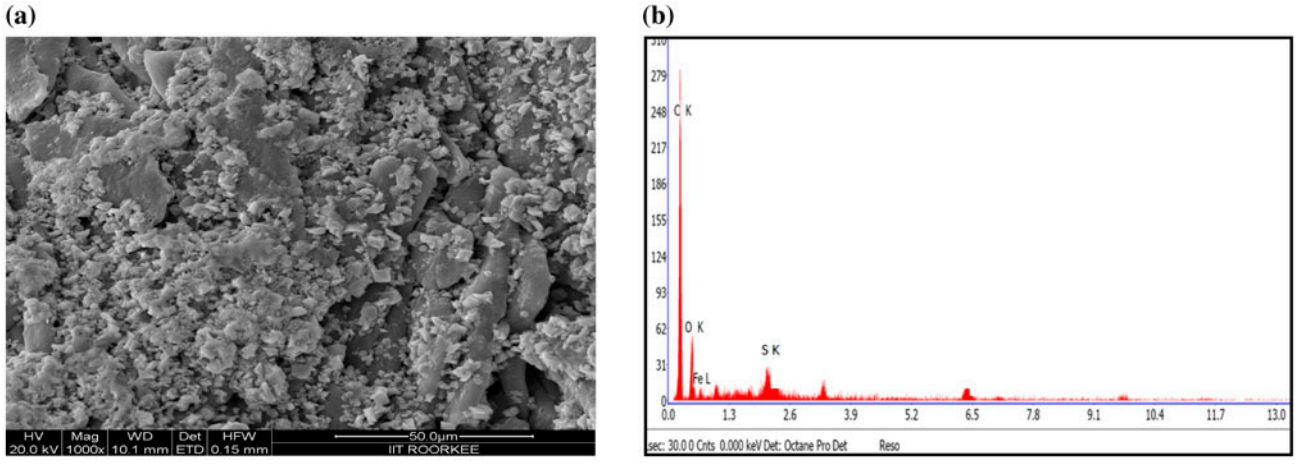

Fig. 3. (a) SEM image of CSAC after immobilization of micro-organism and (b) EDX analysis of CSAC after immobilization of micro-organism.

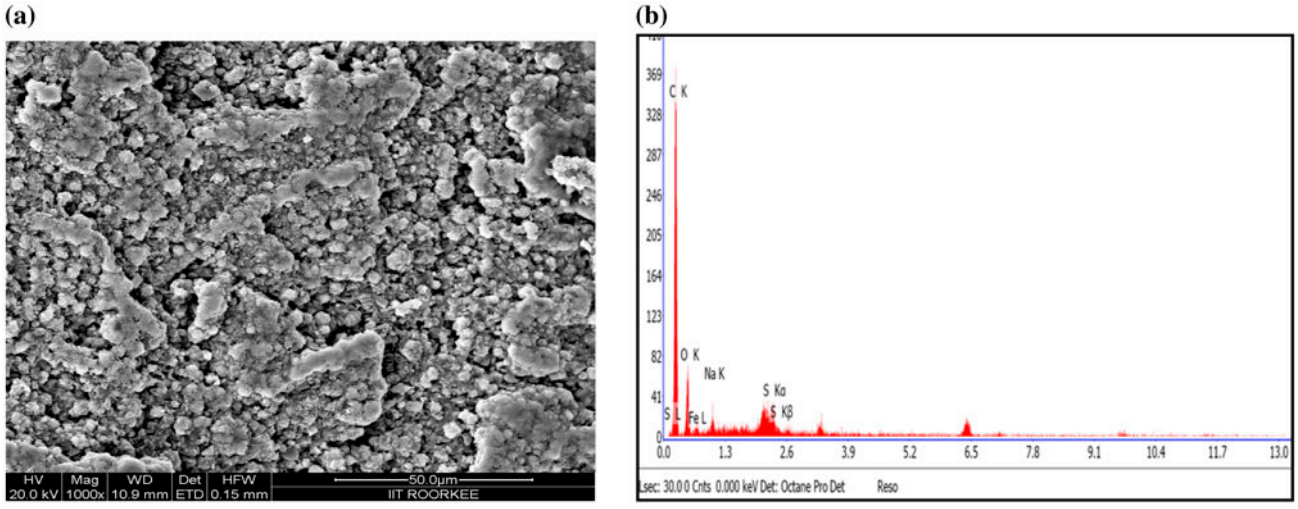

Fig. 4. (a) SEM image of CSAC after simultaneous biosorption and bioaccumulation and (b) EDX analysis of CSAC after simultaneous biosorption and bioaccumulation.

tions of O–H and –N–H functional groups [21,22]. The decrease in peak after immobilization and simultaneous biosorption and bioaccumulation corresponds to the strong hydroxyl group and amide vibrations. Vibrations at 2,921.98 cm^{-1} indicated the occurrence of asymmetric or symmetric CH stretching of aliphatic acids [23]. Peaks between 1,650 and 1,550 cm^{-1}, 1,800 cm^{-1}, 300 cm^{-1} and 1,160 and 1,000 cm^{-1} signified the occurrence of C=C in C=H stretching, aromatic rings, and C–O stretching [24]. Absorbance peaks formed due to weak reflectance at 700–610 cm^{-1} on the surface of CSAC designated the occurrence of –C≡C–H: C–H bend due to alkynes functional group. Occurrence and absence of functional groups on CSAC surface specified that phenol and cyanide biosorption on the surface of CSAC was arbitrated by chemical ion exchange.

3.2. Optimization of process parameters

3.2.1. Influence of biosorbent dose and pH

The influence of CSAC biosorbent dose on the elimination of phenol and cyanide was examined in the range of 5–60 g/L (Fig. 6). Initial concentration of phenol and cyanide in aqueous solution was set constant at 500 and 50 mg/L, respectively. It can be observed from Fig. 6 that at the initial stage, the

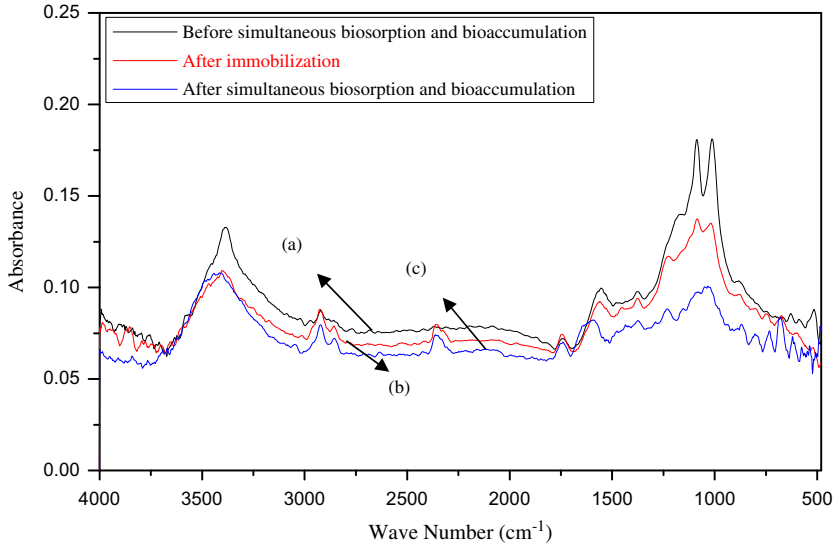

Fig. 5. FTIR spectrum of CSAC: (a) before simultaneous biosorption and bioaccumulation, (b) after immobilization of co-culture and (c) after simultaneous biosorption and bioaccumulation of phenol and cyanide.

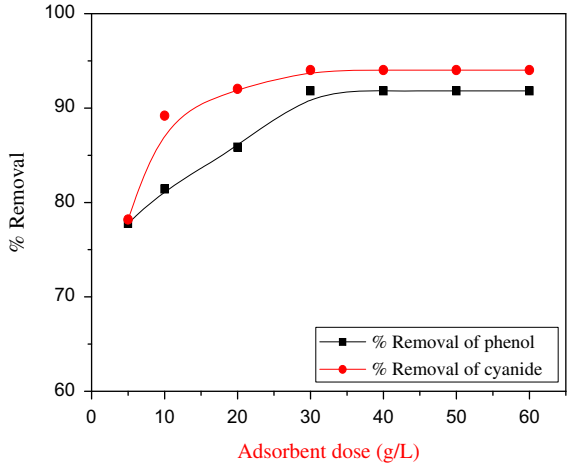

Fig. 6. Influence of dose on percentage removal of phenol and cyanide.

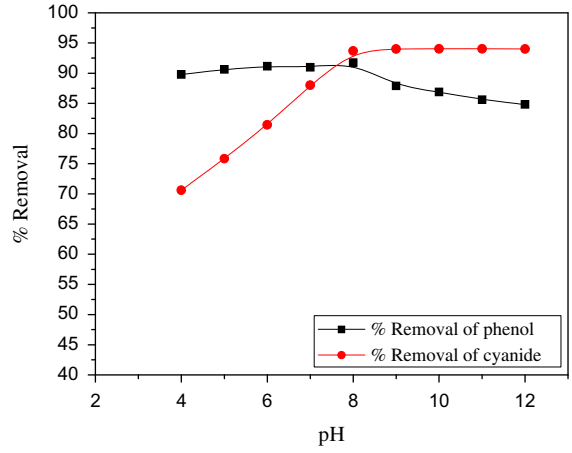

Fig. 7. Influence of pH on percentage removal of phenol and cyanide.

percent removal of phenol and cyanide was higher. The increasing phenol and cyanide removal may be owing to the available surface area of biosorbent and accessibility of vacant sites for biosorption [25]. The percentage removal of phenol and cyanide increased up to 30 g/L. On additional increase in biosorbent dose, the variation in removal percent was very slow. After attaining 91.82% removal for phenol and 94.02% removal for cyanide, biosorbent dose was not considerably effective and percentage removal became constant. Therefore, 30 g/L of CSAC dose is required to attain the maximum percentage removal of phenol and cyanide.

Fig. 7 shows the influence of pH on the simultaneous biosorption and bioaccumulation of phenol and cyanide onto CSAC with biosorbent dose 30 g/L and initial concentration of phenol and cyanide 500 and 50 mg/L, respectively. Initial pH is a significant factor affecting the biosorption capacity of biosorbent. This is recognized to the alteration of the biosorbent surface charge with the variation in pH value. It could be observed that the percentage removal of cyanide increased up to pH increased from 4 to 9, and after that, it became constant at pH higher than 9 [4]. In lower pH range (4–7), there is a sharp reduction in removal percentage of cyanide, which could be due to

hydrolysis of weak acid dissociable cyanides to HCN. Subsequently, HCN is very hydrophilic and its affinity to be adsorbed at low pH is significantly decreased. Though, at higher pH, most of the cyanide exists in undissociated form [4,10,16]. Subsequently, the pK_a value of cyanide is 9.39 and maximum percentage removal of cyanide is acquired in the range of pH 9–12. The removal of phenol is found to be slightly decreased after pH range 8. The phenol pK_a value is 9.9 and the zero-point-charge pH of the CSAC is almost 6.3 [26]. The surface of CSAC biosorbent displays increasingly more negative values with increased pH. At lower values of pH < 6.3, phenol is reserved in the acidic medium and this can be recognized to the positive surface charge of biosorbent and the occurrence of a H^+ ion competing with the phenol for the adsorption sites [27]. At pH more than 8, phenol as a weak acid is incompletely ionized and the negatively charged phenol ions are repelled by the negatively charged biosorbent surface. The decrease in phenol removal of pH more than 8 may also be an outcome of the competition between the phenol anions and OH^- ions [26]. Agrawal et al. [16] predicted the optimum value of pH equal to 8 for *S. odorifera* (MTCC 5700) and Kumar et.al. [17] stated the optimum pH as 7 for removal of phenol by *P. putida* (MTCC 1194). The main reason behind the inequality in optimum pH among bacteria was the difference in functional groups existing on the surface of the cell membrane.

3.2.2. Influence of time and temperature

The influence of contact time on the percentage removal of simultaneous biosorption and bioaccumulation of phenol and cyanide is shown in Fig. 8. It could be understood that the percent removal of phenol and cyanide increased with increase in contact time until an equilibrium was attained at about 44 h for phenol and 42 h for cyanide. The maximum rate of percent removal at the initial stage was owing to availability of surface area of biosorbent and afterward the biosorbent capacity becomes exhausted (i.e. at equilibrium) and continuous reduction in the concentration driving force [28]. The maximum phenol removal from aqueous solution was 91.74%, whereas the maximum cyanide removal was found 94.04%, demonstrating that the CSAC influenced a high attraction for both phenol and cyanide.

Fig. 9 indicates the influence of temperature on phenol and cyanide biosorption. The percentage removal of phenol and cyanide observed in the temperature range from 20 to 40°C. Though, the percentage removal was found more at temperature ranged from 20 to 30°C and turn out to be more stable on additional increase in the temperature. With increasing temperature, the solution viscosity starts to decrease, thereby increasing the adsorbate diffusion rate within the pores [29]. Mostly, the rise in temperature in the sorption of pollutants on the surface of the biosorbent increases the number of active sites by breaking the bonds present in cell walls [30,31]. The initial increase in biosorption of cyanide with increase in temperature is maybe owing to increase in active sites resulting from the breaking of some of the internal bonds nearby the edge of the active surface sites of the biosorbent [32]. Similar results for biosorption onto modified activated carbon was obtained by Canizares [33]. Binding of phenol and cyanide as a linear function of temperature showed the involvement of chemical forces as well as physical forces of adsorption. It could be concluded from figure that percentage removal of phenol and cyanide does not differ

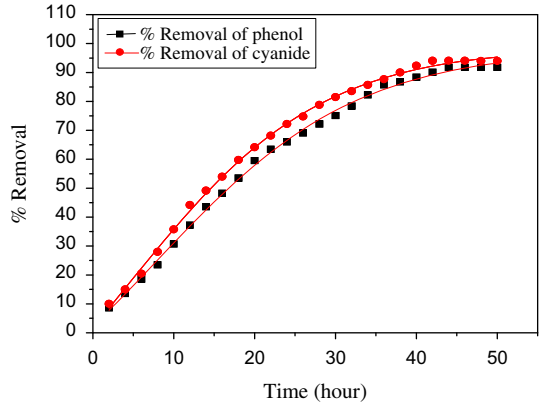

Fig. 8. Influence of contact time on percentage removal of phenol and cyanide.

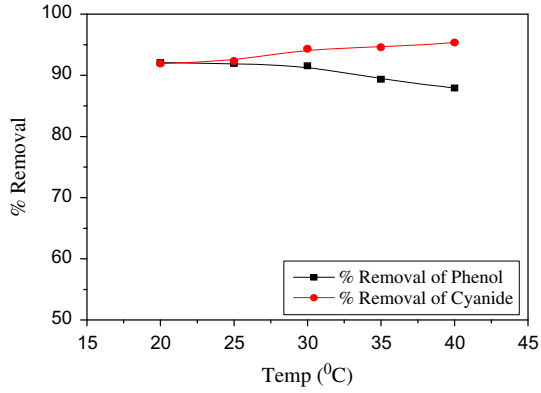

Fig. 9. Influence of temperature on percentage removal of phenol and cyanide.

significantly with changes in temperature (20–40˚C). In this study, additional thermodynamic modeling study was carried out to explain the influence of temperature on biosorption of phenol and cyanide.

3.2.3. Influence of initial concentration of phenol and cyanide

The biosorption of phenol and cyanide was calculated experimentally by changing the initial concentrations of phenol from 100 to 1,000 mg/L and cyanide from 10 to 100 mg/L (Fig. 10(a) and (b)). The results demonstrated that the removal of phenol and cyanide reduced with increasing initial concentration. This may be owing to accessibility of enough number of vacant sites onto the surface of CSAC to absorb phenol and cyanide. Specific uptake for phenol increases from 3.32 to 27.48 mg/g of biosorbent and for cyanide from 0.33 to 3.03 mg/g of biosorbent; however, percentage removal decreases from 99.96 to 82.46% for phenol and from 99.99 to 90.97% for cyanide with increasing initial concentration 100–1,000 mg/L for phenol and 10–100 mg/L for cyanide.

3.3. Isotherm modeling

Equilibrium modeling of biosorption data is essential for defining the interactive behavior of biosorbents and adsorbates. Distribution of pollutants between the solid phase (biosorbent) and liquid phase can be described by several monocomponent and binary component equilibrium isotherm models.

3.3.1. Monocomponent modeling

The monocomponent biosorption existences were expressed by the non-competitive model. Several isotherm models like Langmuir, Freundlich, Redlich–Peterson, Tóth, and Fritz–Schlunder have been used to explain the monocomponent isotherm equilibrium features of biosorption of phenol and cyanide onto CSAC [34,35]. The experimental biosorption equilibrium data were acquired by changing the phenol and cyanide concentration with a fixed dose of CSAC (30 g/L).
The model equations are given below:
Langmuir:

$$q_e = (Q_0\, b\, C_e)/(1 + b\, C_e) \tag{4}$$

Freundlich:

$$q_e = K_F\, C_e^{1/n} \tag{5}$$

Redlich–Peterson:

$$q_e = K_{RP} \cdot C_{eq}/1 + a_{RP} \cdot C_{eq}^{\beta} \tag{6}$$

Tóth:

$$q_e = q_e^{\infty} \cdot C_{eq}/(a + C_{eq}^{n})^{1/n} \tag{7}$$

Fritz–Schlunder:

$$q_e = \alpha_1 \cdot C_{eq}^{\beta_1}/1 + \alpha_2 \cdot C_{eq}^{\beta_2} \tag{8}$$

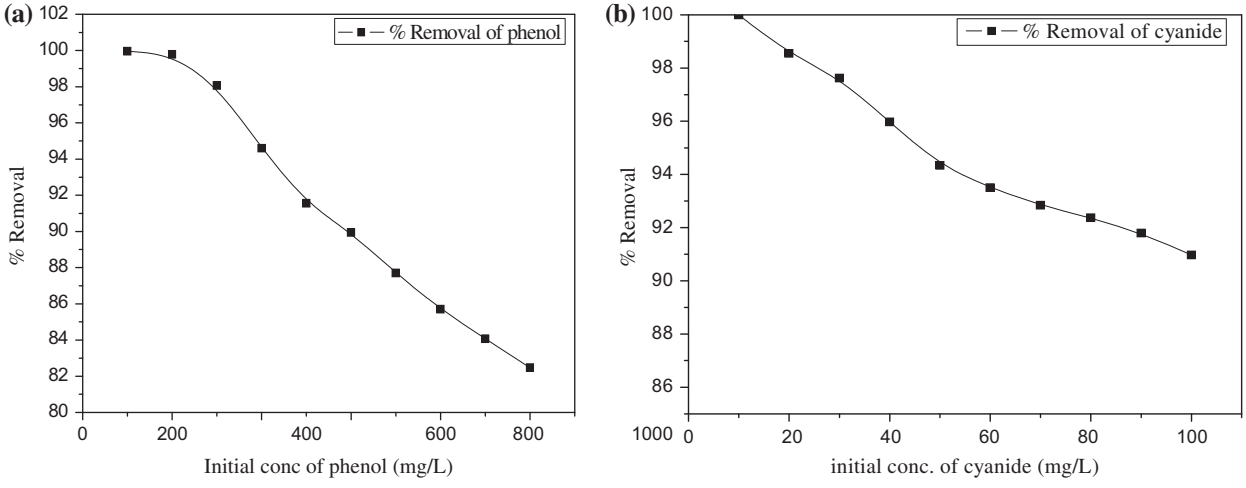

Fig. 10. (a) Influence of initial concentration of phenol on percentage removal and (b) influence of initial concentration of cyanide on percentage removal.

In a Langmuir isotherm model equation, b is the adsorption equilibrium constant. It is associated with the free energy of biosorption and heterogeneity measurement of the biosorption process. Q_0 is the maximum amount of pollutant per unit weight of biosorbent to form a complete monolayer on the surface bound at high C_e, and b is a constant related to the affinity of the binding sites.

The Freundlich expression is an empirical equation based on adsorption on a heterogeneous surface, signifying that binding sites are not equivalent and/or independent. Where K_F and n are the monocomponent Freundlich constant characteristics of the system [36]. Redlich–Peterson model combines the elements of the Langmuir and Freundlich model in an equation (6), where K_{RP} and a_{RP} are the constants of Redlich–Peterson isotherm model and b is the isotherm exponent which lies between 0 and 1 [36]. The Tóth and Fritz–Schlunder models are not commonly used to define biosorption of phenol and cyanide onto CSAC.

The main purpose to obtain monocomponent biosorption studies is to estimate the suitable model on the basis of lower MPSD and to evaluate the parameters of the multicomponent models used in biosorption studies. The model parameters were obtained by non-linear least-squares regression analysis techniques.

The best equilibrium isotherm model is obtained on the basis of bias factor (B_F) nearer to unity and low values of statistical indices such as normalized standard deviation (NSD) and root mean square error (RMSE). The isotherm model parameters for phenol and cyanide are shown in Table 1. The value of bias factor (B_F), statistical indices NSD, and RMSE values are given in Table 2. Figs. 11(a) and (b) offer the comparison between the five different monocomponent isotherm models for phenol and cyanide. Biosorbent has a heterogeneous surface for the biosorption of phenol and cyanide. So, it is predictable that the Redlich–Peterson model and Freundlich isotherm model equations can well characterize the experimental equilibrium sorption data. The MPSD values are lower for the Freundlich and the Redlich–Peterson models than that for the Langmuir, Tóth, and Fritz–Schlunder model. Consequently, the equilibrium biosorption data for simultaneous biosorption and bioaccumulation on CSAC can be considered suitable by the Freundlich and the Redlich–Peterson models in the calculated concentration range.

Between the two parameter model, the Freundlich model gives a better fit than the Langmuir model. The

Table 1
Mono- and binary component model parameters for simultaneous biosorption and bioaccumulation of phenol and cyanide onto CSAC

Adsorbate	Langmuir model			Freundlich model			Redlich–Peterson model			
	Q_o (mg/g)	b	MPSD	K_F (mg/g)	n	MPSD	K_{RP} (L/g)	a_{RP} (L/mg)	β	MPSD
Phenol	15.27	3.58	36.66	7.15	4.15	10.08	174,660	24,341.46	0.76	10.09
Cyanide	2.43	1.39	37.71	1.30	4.01	17.18	469,365	371,399	0.75	17.41

Adsorbate	Tóth model				Fritz–Schlunder model				
	q_{to}	a	n	MPSD	α_1 ((mg/g)/(mg/L)$^{\beta 1}$)	α_2 ((mg/L)$-\beta 2$)	β_1	β_2	MPSD
Phenol	9,815.99	0.33	0.04	11.30	4.36	0.01	0.24	−0.0004	10.08
Cyanide	7,114.30	0.31	0.03	19.37	0.05	−0.93	0.09	0.02	11.45

Adsorbate	Non modified Langmuir	Modified Langmuir		Extended Langmuir		
	MPSD	$\eta_{i,j}$	MPSD	$Q_{o,i}$ (mg/g)	b_i	MPSD
Phenol	104.60	13.46	67.50	500.55	0.003	12.37
Cyanide	103.83	0.60	68.10	2.41	1.26	19.20

Adsorbate	Extended Freundlich				Non modified Redlich–Peterson model	Modified Redlich–Peterson model	
	x_i	y_i	z_i	MPSD	MPSD	$n_{i,j}$	MPSD
Phenol	0.01	0.02	−0.04	10.85	106.01	6.37	38.77
Cyanide	−0.10	−0.001	−2.21	16.31	27.34	38.99	72.65

Table 2
Statistical indices values of phenol and cyanide onto CSAC

S. no.	Models	Phenol			Cyanide		
		Bf	NSD	RMSE	Bf	NSD	RMSE
1	Langmuir model	0.84	32.79	6.28	0.001	33.73	0.24
2	Freundlich model	0.99	9.02	1.48	0.07	15.37	0.16
3	Redlich–Peterson model	0.99	9.02	1.49	0.94	15.57	0.19
4	Toth model	0.98	10.11	1.10	0.95	17.32	0.13
5	Fritz–Schlunder model	0.99	9.02	0.89	0.98	10.24	0.10

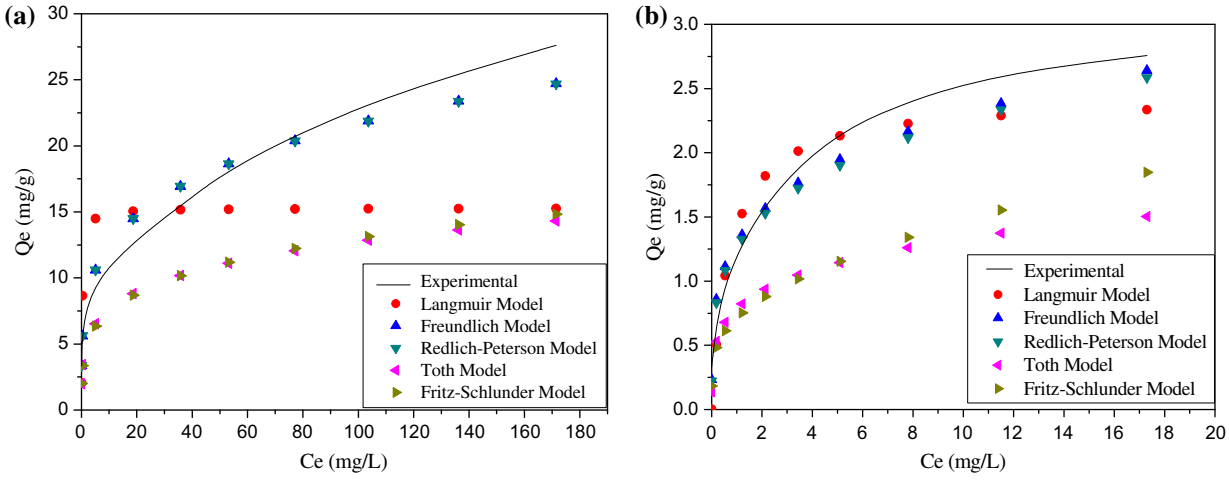

Fig. 11. (a) Comparison of monocomponent isotherm model for phenol and (b) comparison of monocomponent isotherm model for cyanide.

greater the value of n, the greater the affinity and the more heterogeneity of the sites of biosorbent will be greater. It is established from Table 1 that the CSAC shows little more heterogeneity for phenol than that for cyanide; as a result, both phenol and cyanide are well adsorbed by CSAC. In the favorable biosorption process, the value of constant n in Freundlich model should be between 1 and 10. Table 1 shows the value of n obtained between 1 and 10 for phenol as well as for cyanide, representing that the biosorption of both phenol and cyanide is favorable onto surface of CSAC [36].

The value of the Redlich–Peterson model constant β between 0 and 1 shows a favorable biosorption process onto CSAC. The values of β for phenol and cyanide are established to be 0.76 and 0.75, respectively. Therefore, both phenol and cyanide are adsorbed satisfactorily. Thus, both equilibrium isotherm models, viz., Redlich–Peterson and Freundlich, show the same conclusion. In the Langmuir isotherm model, the value of constant b indicates the feasibility of biosorption process over the determination of dimensionless separation factor R_L [37], which is defined as:

$$R_L = 1/(1 + b C_0) \tag{9}$$

Here, C_0 is the initial concentration of adsorbate (g/l), and b is the Langmuir constant (l/g).

This demonstrates the nature of biosorption as $R_L = 1$ (linear), $R_L = 0$ (irreversible), $0 < R_L < 1$ (favorable), and $R_L > 1$ (unfavorable). The values of R_L for biosorption of phenol and cyanide onto CSAC are in favorable range. In this study, the value of R_L has been found less than 1 for both phenol and cyanide presenting that the biosorption of phenol and cyanide onto CSAC is very favorable. The value of R_L is found to be decreased with increasing initial concentration of phenol and cyanide [38]. Based on the results indicated in Table 1, best-fitted isotherm models for phenol biosorption are determined in the increasing order: (Freundlich > Fritz–Schlunder > Redlich–Peterson >Tóth > Langmuir) and for cyanide in the order: (Fritz–Schlunder > Freundlich > Redlich–Peterson > Tóth >Langmuir).

3.3.2. Binary component isotherm modeling

When more than one component is existing, competition and interference occurrences for sites available for biosorption take place and lead to an additional difficult mathematical origination of the equilibrium. The simultaneous biosorption data of phenol and cyanide from the binary mixture onto CSAC has been fitted to the numerous multicomponent equilibrium isotherm models, such as non-modified Langmuir and modified Langmuir models, extended Langmuir and Freundlich models, and non-modified Redlich–Peterson and modified Redlich–Peterson models. Multicomponent model equations are given below [39–41]:

Non-modified competitive Langmuir:

$$q_{e,i} = (Q_{0,i} b_i C_{e,i})/(1 + \sum_{j=1}^{N} b_j C_{e,j}) \quad (10)$$

Modified competitive Langmuir:

$$q_{e,i} = (Q_{0,i} b_i C_{e,i}/n_i)/(1 + \sum_{j=1}^{N} b_j (C_{e,j}/n_j)) \quad (11)$$

Extended Langmuir:

$$q_{e,i} = (Q_{0,i} b_i C_{e,i})/(1 + \sum_{j=1}^{N} b_j C_{e,j}) \quad (12)$$

Extended Freundlich:

$$q_{e,i} = (K_{F,i} C_{e,i}^{1/ni+xi})/(C_{e,i}^{xi} + y1 C_{e,j}^{z,i}) \quad (13)$$

$$q_{e,j} = (K_{F,j} C_{e,j}^{1/nj+xj})/(C_{e,j}^{xj} + y2 C_{e,i}^{z,j}) \quad (14)$$

Non-modified competitive Redlich–Peterson model:

$$q_{e,i} = K_{\mathrm{RP}_i} \cdot C_{\mathrm{eq}_i}/1 + \sum_{j=1}^{N} a_{\mathrm{RP}_j} (C_{\mathrm{eq}_j})^{\beta_j} \quad (15)$$

Modified Redlich–Peterson model:

$$q_{e,i} = K_{\mathrm{RP},i} \cdot \left(\frac{C_{\mathrm{eq},i}}{\eta_{\mathrm{RP},i}}\right) \Big/ 1 + \sum_{j=1}^{N} a_{\mathrm{RP},i} \left(\frac{C_{\mathrm{eq},i}}{\eta_{\mathrm{RP},i}}\right)^{\beta_j} \quad (16)$$

For the binary isotherm study, a binary mixture of phenol and cyanide was taken, and simultaneous equilibrium data were calculated by contacting phenol and cyanide solutions of initial concentration, i.e. 100-1,000 mg/L of phenol, and initial concentration of cyanide varied from 10 to 100 mg/L with the CSAC over an equilibrium time of 50 h.

The results of binary component equilibrium isotherm study demonstrate that for 500 mg/L concentration of phenol with the presence of 50 mg/L of cyanide Q_{ph} was 15.26 mg/g. Similarly, for 1,000 mg/L concentration of phenol with the presence of 100 mg/L of cyanide, Q_{ph} was 27.49 mg/g for CSAC. The adsorption capacity of competitive biosorption is reduced due to its dependence on the initial concentration of the pollutants, the surface structure of the biosorbents, and the molecular structure of the competing adsorbate [42].

The MPSD values between the calculated and experimental values for the complete data-set of phenol and cyanide are specified in Table 1, while the plots shown in Figs. 12(a) and (b) revealed the comparison between six multicomponent isotherm models for phenol and cyanide. In binary component system, non-modified Langmuir model demonstrates a poor fit to the equilibrium experimental data with MPSD value 104.60 for phenol and 103.83 for cyanide. Non-modified R–P Model also indicates a poor fit for phenol with high MPSD value 106.01. The values of interaction term $\eta_{i,j}$ in the modified Langmuir model and modified Redlich–Peterson Model were provided lower MPSD value. The interaction term $\eta_{i,j}$ enhanced the fit of the modified Langmuir and Redlich–Peterson model. The extended Langmuir and extended Freundlich models fitted to the experimental data for a binary component system of phenol and cyanide onto CSAC reasonably well. Though, the extended Freundlich model indicates best fitted to the equilibrium experimental data with the lowest value of MPSD 10.85 for phenol and 16.31 for cyanide comparing to other models.

Based on the results indicated in Table 1, best-fitted binary component isotherm models for phenol biosorption are determined in the increasing order: (extended Freundlich > extended Langmuir > Modified Redlich–Peterson > Modified Langmuir > Non-Modified Redlich–Peterson > Non-Modified Langmuir) and for cyanide in the order: (extended Freundlich > extended Langmuir > Non-Modified Redlich–Peterson > Modified Langmuir > Modified Redlich–Peterson > Non-Modified Langmuir). This is estimated as CSAC, has a heterogeneous surface, and biosorption of the monocomponent have been well characterized by the Freundlich isotherm model and binary component data have also been well characterized by the extended Freundlich isotherm model.

In binary component aqueous solution, the components present in aqueous solution may have three types of sorption interaction effects such as: if the

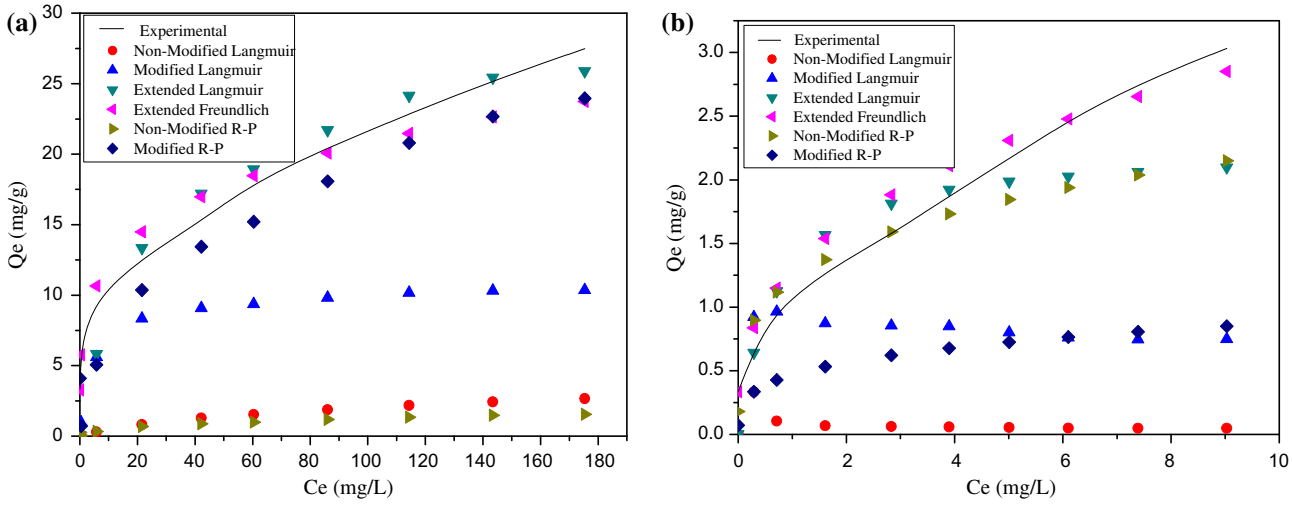

Fig. 12. (a) Comparison of binary component isotherm model for phenol and (b) comparison of binary component isotherm model for cyanide.

adsorption of the adsorbate decreases when there are additional adsorbates present in the multicomponent mixture (antagonism: $Q_{mix}/Q_i < 1$), the adsorption of the adsorbate increases when there are another adsorbates present in the multicomponent mixture (synergism: $Q_{mix}/Q_i > 1$) and if the multicomponent mixture has no effect on the adsorption of each adsorbate (non-interaction: $Q_{mix}/Q_i = 1$) [43].

where Q_i is the biosorption capacity of component present alone in the solution and Q_{mix} is the biosorption capacity of one component in the presence of the other component in binary component aqueous solution.

In this study, the ratio of Q_{mix}/Q_i for phenol and cyanide was calculated as 32.77 and 0.99, respectively, hence founding the fact that phenol and cyanide show synergism and antagonism effects, respectively.

3.3.3. Validation of model

The parameters of monocomponent models are obtained using the non-linear regression analysis method, and statistical indices values of phenol and cyanide for the monocomponent isotherm models are presented in Table 2.

For the monocomponent system to obtain courtesy of the fit of experimental data, the following statistical measure between the experimental and calculated values was used as follows [44]:

$$B_{Fac} = 10\left(\sum \log_{10}(Q_{e,cal}/Q_{e,exp})/N\right) \quad (17)$$

$$NSD = \sqrt{\frac{\sum \left(1 - Q_{e,cal}/Q_{e,exp}\right)^2}{N}} \times 100 \quad (18)$$

$$RMSE = \sqrt{\frac{\sum \left(Q_{e,exp} - Q_{e,cal}\right)^2}{N}} \quad (19)$$

The Marquardt's percent standard deviation (MPSD) error function was used to correlate the experimental, and calculated values for isotherm models are given below:

$$MPSD = 100\sqrt{\frac{1}{n-p}\sum_{i=1}^{p}\left(\frac{Q_{e,i}^{exp} - Q_{e,i}^{cal}}{Q_{e,i}^{exp}}\right)^2} \quad (20)$$

The best fit of the experimental data to the proposed kinetic models is usually shown by lower ARE values [45]:

$$ARE = 100/n\sqrt{\sum_{i=1}^{p}\left(\frac{Q_{e,i}^{exp} - Q_{e,i}^{cal}}{Q_{e,i}^{exp}}\right)^2} \quad (21)$$

where $Q_{e,i}^{exp}$ is the experimental q_e and $Q_{e,i}^{cal}$ is the equivalent calculated q_e according to kinetic model, n is the number of observations.

3.4. Kinetic modeling

In the present study, the calculated values of kinetic models for simultaneous biosorption and

bioaccumulation of phenol and cyanide onto CSAC are studied. The pseudo-first-order and second-order kinetic model are stated as:

$$\text{Lagergren's pseudo-first-order} = q_t = q_e(1 - \exp(-K_1 t)) \quad (22a)$$

where K_1 is the pseudo-first-order adsorption rate constant (h^{-1}).

$$\text{Pseudo-second-order} = q_t = k_2 q_e^2 t/(1 + q_e K_2 t) \quad (22b)$$

where K_2 is the pseudo-second-order adsorption rate constant (g mg^{-1} h^{-1}).

Here, q_t and q_e are the amounts of phenol and cyanide adsorbed per unit mass of biosorbent at time t and at equilibrium, respectively, and can be calculated by Eqs. (1) and (2).

To determine the kinetic model parameters, kinetic experiments were attended at five initial concentrations of phenol:cyanide (100:10, 200:20, 300:30, 500:50, and 1,000:100 mg/L), with the temperature at 30°C, biosorbent dose at 30 g/L, and constant pH of solution at 8. Figs. 13(a) and (b) show the experimental q_t vs. time plots for phenol and cyanide at different initial concentrations, respectively. It can be detected from figure that the biosorption capacity of both components was increasing with time until a certain level where no additional phenol and cyanide is eliminated from the solution. For all phenol and cyanide concentrations, the maximum of phenol and cyanide is eliminated within the first 32 h. It should be observed that an increase in the initial concentration of phenol and cyanide leads to an increase in the biosorption capacity of both component phenol and cyanide by CSAC.

The value of the error function ARE and constants of kinetic models, pseudo-first-order and pseudo-second-order at various initial phenol and cyanide concentrations are given in Tables 3a and 3b.

Lower ARE value indicates the better fit of experimental data. Tables 3a and 3b demonstrate the values of kinetic model constant K_1, K_2, $q_{t(exp)}$, $q_{t(cal)}$, and ARE for phenol and cyanide. The results show that the value of ARE for both phenol and cyanide is lower in case of pseudo-first-order kinetic model in comparison

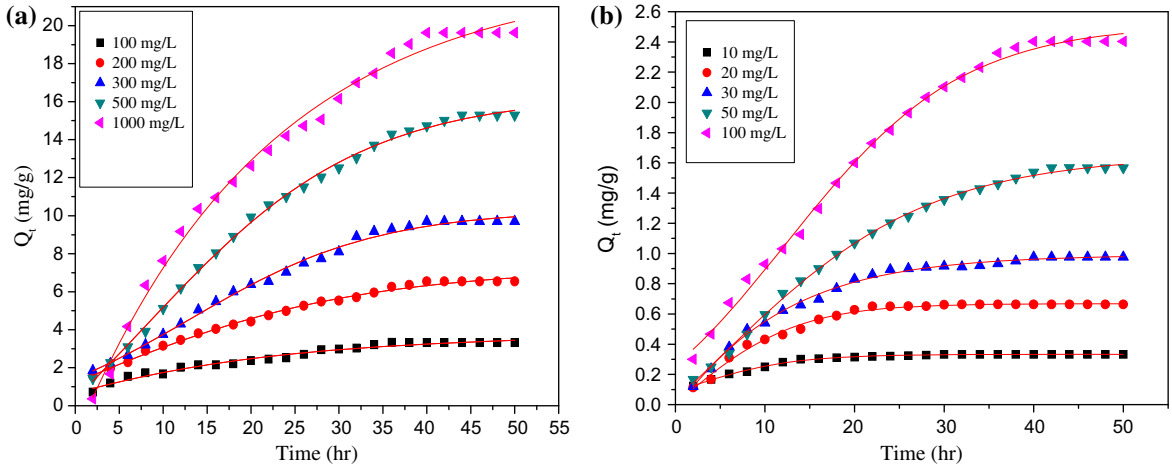

Fig. 13. (a) Concentration–time profile for phenol and (b) concentration–time profile for cyanide.

Table 3a
Kinetic model parameters for phenol

Concentration of phenol	Pseudo-first-order kinetic constant				Pseudo-second-order kinetic constant			
	K_1 (h^{-1})	$q_{t(exp)}$ (mg/g)	$q_{t(cal)}$ (mg/g)	ARE	K_2 (h^{-1})	$q_{t(exp)}$ (mg/g)	$q_{t(cal)}$ (mg/g)	ARE
100	0.095	3.32	3.13	2.11	0.02	3.32	3.92	2.48
200	0.075	6.54	6.35	2.21	0.01	6.54	8.19	2.76
300	0.05	9.70	10.74	2.17	0.002	9.70	15.27	2.22
500	0.029	15.29	21.29	1.10	0.0005	15.29	34.68	1.16
1,000	0.02	18.11	42.11	4.20	7.41E-05	18.11	78.05	8.58

Table 3b
Kinetic model parameters for cyanide

Concentration of cyanide	Pseudo-first-order kinetic constant				Pseudo-second-order kinetic constant			
	K_1 (h^{-1})	$q_{t(exp)}$ (mg/g)	$q_{t(cal)}$ (mg/g)	ARE	K_2 (h^{-1})	$q_{t(exp)}$ (mg/g)	$q_{t(cal)}$ (mg/g)	ARE
10	0.18	0.33	0.33	1.11	0.58	0.33	0.38	1.73
20	0.088	0.66	0.70	1.34	0.08	0.66	0.93	1.85
30	0.07	0.98	1.04	0.94	0.04	0.98	1.45	1.41
50	0.04	1.57	1.99	1.14	0.01	1.57	3.13	1.25
100	0.04	2.40	2.88	1.69	0.01	2.40	4.16	1.80

to ARE in case of pseudo-second-order kinetic model. According to these results, it can be recognized that the pseudo-first-order kinetic model indicates a better correspondence for the biosorption of phenol and cyanide onto CSAC.

3.5. Thermodynamic modeling

Thermodynamic modeling parameters such as the change in entropy (Δs°), change in enthalpy (Δh°), and Gibbs free energy (ΔG°) related to the biosorption process are determined using the following equations [46,47]:

$$\ln k = \frac{\Delta s}{R} - \frac{\Delta h}{RT} \tag{23}$$

$$\Delta G^\circ = -RT \ln k \tag{24}$$

where R is the gas constant = 8.314×10^{-3} kJ/mole/K, ΔG° is kJ/mole, T = temperature in °K, Δs° is kJ/mol K, Δh° is the kJ/mole, and k is the equilibrium constant (amount on biosorbent/amount in solution).

The value of k can be acquired by plotting $\ln(k)$ vs. $1/T$ according to Eq. (23). The parameters of thermodynamic modeling of the phenol and cyanide biosorption onto CSAC are given in Table 4. The value of ΔG° for phenol biosorption was increased from −45.90 to −35.90 kJ/mole and for cyanide biosorption decreased from −104.65 to −126.39 kJ/mole with increasing temperature from 20 to 40°C, signifying that biosorption might be spontaneous at lower temperature for phenol. The negative values of ΔG° were revealed that the biosorption of phenol and cyanide onto CSAC were spontaneous, chemically controlled, and feasible [48]. The value of Δh° for phenol was negative, representing that the biosorption process was exothermic, whereas cyanide biosorption was found to be endothermic in nature. The value of Δs° for phenol and cyanide biosorption onto CSAC was −0.05 kJ/mol K and 0.11 kJ/mol K, respectively. The negative value of Δs° recommended a reduction in degree of freedom of the phenol biosorption [49]. The value of $\Delta s^\circ < 1$ indicates that the process is reversible.

Table 4
Thermodynamic modeling parameters for simultaneous biosorption and bioaccumulation of phenol and cyanide onto CSAC

Adsorbate	Temp. (°C)	CSAC			R^2
		ΔG° (kJ/mole)	Δh° (kJ/mole)	Δs° (kJ/mol K)	
Phenol	20	−45.90	−20.27	−0.05	0.87
	25	−46.14			
	30	−45.60			
	35	−39.31			
	40	−35.90			
Cyanide	20	−104.66	22.52	0.11	0.94
	25	−107.78			
	30	−117.30			
	35	−120.45			
	40	−126.39			

4. Conclusions

In this current study, a simultaneous biosorption and bioaccumulation system was selected for elimination of phenol and cyanide using co-culture/mixed culture immobilized onto CSAC. In conclusion, CSAC had features that were superior for the elimination of phenol and cyanide from the aqueous medium. Several monocomponent and binary component biosorption isotherm models were used to compare the experimental data for phenol and cyanide in both single and in combination. Hence, a binary component system was established better than a monocomponent biosorption system for the elimination of phenol and cyanide. A synergistic effect was exhibited for phenol, whereas antagonism effects were exhibited for cyanide, in the binary component system. The pseudo-first-order kinetic model was indicated a better correspondence for the biosorption of phenol and cyanide. Additionally, the biosorption of phenol onto CSAC indicates exothermic and cyanide indicates endothermic in the nature of the process. These outcomes remark that co-culture/mixed culture immobilized onto CSAC can be appropriately used for the elimination of phenol and cyanide comprising wastewater.

Acknowledgment

The authors acknowledge deepest thanks to Department of chemical engineering, and Institute Instrumentation Center, IITR, Roorkee, India, for providing technical support and facilities. The authors would also like to thank to Ministry of Human Resource Development (MHRD, New Delhi), Government of India for funding this research work.

Nomenclature

q_t	—	uptake of phenol and cyanide at time t (mg/g)
C_t	—	liquid phase concentration of phenol and cyanide at time t (h)
C_i	—	initial pollutant concentration (mg/L)
C_{eq}	—	concentration of adsorbate at equilibrium (mg/L)
V	—	volume of the solution (L)
M	—	weight of the adsorbent (gm)
q_e	—	specific uptake of adsorbent at equilibrium (mg/g)
Q_o	—	Langmuir model constant (mg/g)
B	—	Langmuir model constant
$Q_{e,i}$	—	amount of ith component adsorbed per gram of adsorbent at equilibrium (mg/g)
$Q_{o,i}$	—	constant in modified Langmuir model for ith component (mg/g)
$C_{e,i}$	—	concentration of ith component in the binary mixture at equilibrium (mg/L)
K_F	—	Freundlich model constant (mg/g)
N	—	Freundlich, Toth model constant
$K_{F,i}$	—	extended Freundlich model constant (mg/g)
K_{RP}	—	Redlich–Peterson model constant (L/g)
a_{RP}	—	Redlich–Peterson model constant (L/mg)
β	—	Redlich–Peterson model constant
$\eta_{RP,i}$	—	binary component Redlich–Peterson model constant (L/g)
$a_{RP,i}$	—	binary component Redlich–Peterson model constant (L/mg)
β_j	—	binary component Redlich–Peterson model constant
x_i, y_i, z_i	—	constant in modified Redlich—Peterson model
K_1	—	pseudo-first-order model constant
K_2	—	pseudo-second-order model constant
ΔG°	—	change in Gibbs free energy (kJ/mole)
Δs°	—	change in entropy (kJ/mol K)
Δh°	—	change in enthalpy (kJ/mole)
B_F	—	Bias factor
NSD	—	normalized standard deviation
RMSE	—	root mean square error
ARE	—	average relative error
MPSD	—	Marquardt's percent standard deviation
N	—	number of observations in the experimental isotherm
P	—	number of parameter in regression model
$Q_{e,i}^{exp}$	—	experimental value of Q_e (mg/g)
$Q_{e,i}^{cal}$	—	predicted value of Q_e (mg/g)
α_1	—	constant in Fritz–Schlunder isotherm $(mg/g)/(mg/L)^{\beta 1}$
α_2	—	constant in Fritz–Schlunder isotherm $(mg/L)^{-\beta_2}$
$\beta_1\beta_2$	—	constants in Fritz–Schlunder isotherm

References

[1] Z. Aksu, J. Yener, A comparative adsorption/biosorption study of mono-chlorinated phenols onto various sorbents, Waste Manage. 21 (2001) 695–702.
[2] G. Busca, S. Berardinelli, C. Resini, L. Arrighi, Technologies for the removal of phenol from fluid streams: A short review of recent developments, J. Hazard. Mater. 160 (2008) 265–288.
[3] N. Calace, E. Nardi, B.M. Petronio, M. Pietroletti, Adsorption of phenols by papermill sludges, Environ. Pollut. 118 (2002) 315–319.
[4] R.R. Dash, A. Gaur, C. Balomajumder, Cyanide in industrial wastewaters and its removal: A review on biotreatment, J. Hazard. Mater. 163 (2009) 1–11.
[5] J.D. Desai, C. Ramakrishna, Microbial degradation of cyanides and its commercial application, J. Sci. Ind. Res. 57 (1998) 441–453.

[6] Y.B. Patil, K.M. Paknikar, Biodetoxification of silver-cyanide from electroplating industry wastewater, Lett. Appl. Microbiol. 30 (2000) 33–37.
[7] J.R. Rao, T. Viraraghavan, Biosorption of phenol from an aqueous solution by *Aspergillus niger* biomass, Bioresour. Technol. 85 (2002) 165–171.
[8] ATSDR, Agency for toxic substances and Disease Registry, Public Health Statement, Cyanide. Available from: <http://www.atsdr.cdc.gov/toxprofiles/tp.asp?id=72&tid=19.2006>.
[9] ATSDR, Agency for toxic substances and Disease Registry, Toxicological profile for phenol, US, Department of Health and Human Service. Available from: <<http://www.atsdr.cdc.gov/toxprofiles/tp.asp?id=148&tid=27>.2008>.
[10] V. Mishra, C. Balomajumder, V.K. Agarwal, Kinetics, mechanistic and thermodynamics of Zn(II) ion sorption: A modeling approach, Clean—Soil Air Water 40 (2012) 718–727.
[11] A.E. Perrotti, C.A. Rodman, Factors involved with biological regeneration of activated carbon, AlChE Symp. Ser. 70 (1974) 316–325.
[12] I.K. Kapdan, F. Kargi, Simultaneous biodegradation and adsorption of textile dyestuff in an activated sludge unit, Process Biochem. 37 (2002) 973–981.
[13] A. Mordocco, C. Kuek, R. Jenkins, Continuous degradation of phenol at low concentration using immobilized *Pseudomonas putida*, Enzyme Microb. Technol. 25 (1999) 530–536.
[14] O.S. Amuda, A.A. Giwa, I.A. Bello, Removal of heavy metal from industrial wastewater using modified activated coconut shell carbon, Biochem. Eng. J. 36 (2007) 174–181.
[15] O.A. Sodeinde, Preparation of a locally produced activated carbon from coconut shells and its use in reducing hexamine cobalt (III), Intl. J. Chem. Eng. Appl. 3 (2012) 67–71.
[16] B. Agrawal, C. Balomajumder, Coke waste water: A source of phenol and cyanide assimilating bacteria, J. Sci. Technol. Manage. 5 (2012) 2012.
[17] A. Kumar, S. Kumar, S. Kumar, Biodegradation kinetics of phenol and catechol using *Pseudomonas putida* MTCC 1194, Biochem. Eng. J. 22 (2005) 151–159.
[18] G. Kotturi, C.W. Robinson, W.E. Inniss, Phenol degradation by a psychrotrophic strain of *Pseudomonas putida*, Appl. Microbiol. Biotechnol. 34 (1991) 539–543.
[19] V. Turon, C. Baroukh, E. Trably, E. Latrille, E. Fouilland, J.P. Steyer, Use of fermentative metabolites for heterotrophic microalgae growth: Yields and kinetics, Bioresour. Technol. 175 (2015) 342–349.
[20] D. Pokhrel, T. Viraraghavan, Arsenic removal from an aqueous solution by modified *A. niger* biomass: Batch kinetic and isotherm studies, J. Hazard. Mater. 150 (2008) 818–825.
[21] S.A. Ozcan, S. Tunali, T. Akar, A. Ozacan, Biosorption of lead (II) ions onto waste biomass of *Phaseouls vulgaris* L. Estimation of the equilibrium, kinetic and thermodynamic parameters, Desalination 244 (2009) 188–198.
[22] W. Shen, S. Chen, S. Shi, X. Li, X. Zhang, W. Hu, Adsorption of Cu(II) and Pb(II) onto diethylenetriamine-bacterial cellulose, Carbohydr. Polym. 75 (2009) 110–114.
[23] L. Yao, Z.F. Ye, M.P. Tong, P. Lai, J.R. Ni, Removal of Cr^{3+} from aqueous solution by biosorption with aerobic granules, J. Hazard. Mater. 165 (2008) 250–255.
[24] S. Basha, Z.P.V. Murthy, B. Jha, Sorption of Hg(II) onto Carica papaya: Experimental studies and design of batch sorber, Chem. Eng. J. 147 (2009) 226–234.
[25] I.A.W. Tan, A.L. Ahmad, B.H. Hameed, Adsorption isotherms, kinetics, thermodynamics and desorption studies of 2,4,6-trichlorophenol on oil palm empty fruit bunch-based activated carbon, J. Hazard. Mater. 164 (2009) 473–482.
[26] M. Dai, Mechanism of adsorption for dyes on activated carbon, J. Colloid Interface Sci. 198 (1998) 6–10.
[27] C. Qing, Study on the adsorption of lanthanum(III) from aqueous solution by bamboo charcoal, J. Rare Earth 28 (2010) 125–131.
[28] A. Verma, S. Chakraborty, J.K. Basu, Adsorption study of hexavalent chromium using tamarind hull-based adsorbents, Sep. Purif. Technol. 50 (2006) 336–341.
[29] A.H. Sulaymon, A.A. Mohammed, T.J. Al-Musawi, Competitive biosorption of lead, cadmium, copper, and arsenic ions using algae, Environ. Sci. Pollut. Res. 20 (2013) 3011–3023.
[30] K. Saltalı, A. Sarı, M. Aydın, Removal of ammonium ion from aqueous solution by natural Turkish (Yıldızeli) zeolite for environmental quality, J. Hazard. Mater. 141 (2007) 258–263.
[31] V. Mishra, C. Balomajumder, V.K. Agarwal, Design and optimization of simultaneous biosorption and bioaccumulation (SBB) system: A potential method for removal of Zn(II) ion from liquid phase, Desalin. Water Treat. 51 (2013) 3179–3188.
[32] R.R. Dash, C. Balomajumder, A. Kumar, Removal of cyanide from water and wastewater using granular activated carbon, Chem. Eng. J. 146 (2009) 408–413.
[33] P. Canizares, M. Carmona, O. Baraza, A. Delgado, M.A. Rodrigo, Adsorption equilibrium of phenol onto chemically modified activated carbon F400, J. Hazard. Mater. 131 (2006) 243–248.
[34] R.K. Singh, S. Kumar, S. Kumar, A. Kumar, Development of parthenium based activated carbon and its utilization for adsorptive removal of p-cresol from aqueous solution, J. Hazard. Mater. 155 (2008) 523–535.
[35] A. Kumar, S. Kumar, S. Kumar, D.V. Gupta, Adsorption of phenol and 4-nitrophenol on granular activated carbon in basal salt medium: Equilibrium and kinetics, J. Hazard. Mater. 147 (2007) 155–166.
[36] M.F. Carvalho, A.F. Duque, I.C. Goncalves, P.M.L. Castro, Adsorption of fluorobenzene onto granular activated carbon: Isotherm and bioavailability studies, Bioresour. Technol. 98 (2007) 3424–3430.
[37] K. Kadirvelu, P. Senthilkumar, K. Thamaraiselvi, V. Subburam, Activated carbon prepared from biomass as adsorbent: Elimination of Ni(II) from aqueous solution, Bioresour. Technol. 81 (2002) 87–90.
[38] B.H. Hameed, I.A.W. Tan, A.L. Ahmad, Adsorption isotherm, kinetic modeling and mechanism of 2,4,6-trichlorophenol on coconut husk-based activated carbon, Chem. Eng. J. 144 (2008) 235–244.
[39] Z. Aksu, D. Akpinar, Simultaneous adsorption of phenol and chromium (VI) from binary mixtures onto

powdered activated carbon, J. Environ. Sci. Health. Part A. 3 (2008) 379–405.
[40] S. Kumar, M. Zafar, J.K. Prajapati, S. Kumar, S. Kannepalli, Modeling studies on simultaneous adsorption of phenol and resorcinol onto granular activated carbon from simulated aqueous solution, J. Hazard. Mater. 185 (2011) 287–294.
[41] Y. Sağ, Ü. Açikel, Z. Aksu, T. Kutsal, A comparative study for the simultaneous biosorption of Cr(VI) and Fe(III) on *C. vulgaris* and *R. arrhizus*: Application of the competitive adsorption models, Process Biochem. 33 (1998) 273–281.
[42] J. Ren, C.F. Huo, X.D. Wen, Z. Cao, J.G. Wang, Y.W. Li, H. Jiao, Adsorption of NO, NO_2, pyridine and pyrrole on α-M_2C(0001), Surf. Sci. 601 (2007) 1599–1607.
[43] H.E. Reynel-Avila, D.I. Mendoza-Castillo, V. Hernandez-Montoya, A. Bonilla-Petriciolet, Multicomponent removal of heavy metals from aqueous solution using low-cost sorbents, in: B. Antizar-Ladislao, R. Sheikholeslami, Water Production and Wastewaters Treatment. Nova Science Publications, UK, 2011, pp. 69–99.
[44] E.Z. Panagou, V.S. Kodogiannis, Application of neural networks as a non-linear modelling technique in food mycology, Expert Syst. Appl. 36 (2009) 121–131.
[45] A. Behnamfard, M.M. Salarirad, Equilibrium and kinetic studies on free cyanide adsorption from aqueous solution by activated carbon, J. Hazard. Mater. 170 (2009) 127–133.
[46] M. Ahmaruzzaman, Adsorption of phenolic compounds on low-cost adsorbents: A review, Adv. Colloid Interface Sci. 143 (2008) 48–67.
[47] R.R. Sheha, E. Metwally, Equilibrium isotherm modeling of cesium adsorption onto magnetic materials, J. Hazard. Mater. 143 (2007) 354–361.
[48] I.A.W. Tan, B.H. Hameed, A.L. Ahmad, Equilibrium and kinetic studies on basic dye adsorption by oil palm fibre activated carbon, Chem. Eng. J. 127 (2007) 111–119.
[49] Q. Fu, Y. Deng, H. Li, J. Liu, H. Hu, S. Chen, T. Sa, Equilibrium, kinetic and thermodynamic studies on the adsorption of the toxins *of Bacillus thuringiensis* subsp. kurstaki by clay minerals, Appl. Surf. Sci. 255 (2009) 4551–4557.